Inorganic Chemistry

Article

pubs.acs.org/IC

Synthesis and Characterization of Mid-Infrared Transparency Compounds: Acentric $BaHgS_2$ and Centric $Ba_8Hg_4S_5Se_7$

Kui Wu,[†] Xin Su,[†,‡] Shilie Pan,*[,†] and Zhihua Yang[†]

[†]Key Laboratory of Functional Materials and Devices for Special Environments of CAS; Xinjiang Key Laboratory of Electronic Information Materials and Devices; Xinjiang Technical Institute of Physics & Chemistry of CAS, 40-1 South Beijing Road, Urumqi 830011, China

[‡]University of Chinese Academy of Sciences, Beijing 100049, China

Supporting Information

ABSTRACT: Two mid-IR transparency compounds, namely, acentric $BaHgS_2$ (BHS) and centric $Ba_8Hg_4S_5Se_7$ (BHSSe), were successfully synthesized by a conventional solid-state reaction method. The space group of BHS is orthorhombic $Pmc2_1$ with $[HgS_4]$ tetrahedra and isolated dumbbell-shaped $[HgS_2]$ units, while BHSSe belongs to the orthorhombic space group *Pnma* with infinite isolated $_\infty[HgSe_2(S/Se)_2]^{4-}$ chains. Raman spectra and thermal analysis of the titled materials were measured. In addition, their band gaps are found to be 1.93 (BHS) and 1.98 eV (BHSSe) from the measured diffuse reflectance spectra. Significantly, the powder BHS sample exhibits a good second harmonic generation (SHG) response of ~6.5 times compared with that of reference $AgGaS_2$ at a fundamental wavelength (2.09 μm). The calculated SHG coefficients of BHS are also reported, and the maximum result agrees well with the test observation.

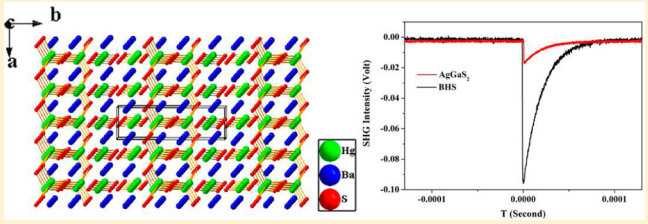

INTRODUCTION

In recent years, lasers play a critical role in the modern technology development and are applied in various fields, such as manufacture, medical treatment, military, and scientific research.[1,2] Nowadays, frequency conversion technology has been developed to expand the fields of laser application. Nonlinear optical (NLO) materials, as one of efficient frequency-shifting devices, have attracted increasing attention.[3−9] As for UV and visible region, many metal oxides have been discovered through various synthetic strategies, such as borates with π-delocalization BO_3 triangles or B_3O_6 groups of the coplanar arrangement, a number of alkaline−alkaline earth carbonate fluorides with π-conjugated CO_3 anionic groups, some of materials containing cations with second-order Jahn−Teller distortions, and other halogen-containing borates, borosilicates, borogermanates, et al.[10−19] However, most of these metal oxides have been limited to be applied in IR region, owing to their short IR cutoff edge. Compared to oxide materials, the outstanding IR NLO materials have been discovered relatively less.[20] Therefore, there still is a huge challenge to find excellent NLO materials with broad IR transparency range, large NLO response, and high damage resistance. After years of exploration and development, now there are many kinds of novel design and synthesis strategies, as follows: (i) numerous alkali metal polychalcogenide fluxes, including polychalcophosphate, polychalcoarsenate, and polychalcostannate, have been demonstrated useful to discover new materials;[21,22] (ii) the d^0 transition-metal cations and main group cations with lone electron pairs (Pb^{2+}, Bi^{3+}, As^{3+}, and Sb^{3+}) are incorporated;[23,24] (iii) some quaternary materials with tetrahedral building blocks have been discovered and have shown good potential;[25] (iv) introducing rare-earth elements (Ln) into metal chalcogenides is also one efficient method for exploring the functional materials.[26] On the basis of these strategies, many new multinary IR materials exhibiting interesting structures and physical properties have been discovered.[21−26]

Recently, the Hg-containing compounds have attracted our interest since Hg is a largely polarizable metal with variable coordination environments and has a great potential to form new special structures, which gives us a new way to design new compounds by introducing the Hg element into chalcogenides.[27] To date, a new family of metal chalcogenides containing the Hg element with outstanding properties was discovered, such as $HgGa_2S_4$ and $A_2Hg_3M_2S_8$ (A = K, Rb; M = Ge, Sn).[28] Theoretical studies also indicate that introducing alkaline-earth metal into structure could effectively broaden the band gap and improve its laser-damaged threshold.[29] These results motivate us to design and synthesize new NLO materials in the alkaline-earth containing metal chalcogenide compounds.

Guided by these ideas, we focused our interest in the Ba−Hg−Q (Q = S or Se) systems, and only a few compounds have been reported, such as $BaHgS_2$, Ba_2HgS_3 and Ba_2HgS_5.[30−32] Among them, $BaHgS_2$ (BHS) was first synthesized in 1981, and its space group was reported as $Pmc2_1$, but its critical optical

Received: December 9, 2014
Published: March 5, 2015

DOI: 10.1021/ic502939g
Inorg. Chem. 2015, 54, 2772−2779

parameters have not been reported, especially the important NLO coefficients and birefringence for IR NLO materials.[30] Hence, in this work, the crystal structure, band structure, and NLO property of the acentric BHS are systemically presented. Moreover, through introducing the Se atoms into the structure of Ba_2HgS_3,[31] a disordered metal chalcogenide, $Ba_8Hg_4S_5Se_7$ (BHSSe), was also obtained in this work, which crystallizes in the orthorhombic space group *Pnma* and has a similar structure with Ba_2HgS_3. Meanwhile, the crystal structure and important physical properties of centric BHSSe compound are also demonstrated.

EXPERIMENTAL SECTION

Synthesis. Raw materials (HgS, Ba, S, and Se) with purity (3N) in this work were used as purchased. The binary starting materials BaS and BaSe were prepared within the sealed quartz tubes evacuated to 1 × 10^{-3} Pa by the high-temperature reactions. **$BaHgS_2$.** The mixtures of BaS (0.169 g, 1 mmol) and HgS (0.233 g, 1 mmol) were loaded into quartz silica tubes (inner diameter: 10 mm, length: 20 mm) in a glovebox with Ar atmosphere, then flame-sealed at a high vacuum of 1 × 10^{-3} Pa. The sealed tubes were put into a muffle furnace and heated to 850 °C in 30 h, kept there for 48 h, and then slowly cooled to 400 °C with a rate of 3 K/h; finally, the muffle furnace was switched off. Many crimson-red crystals existed in the tubes and were still stable in air after several months.

Powder sample of BHS was synthesized by solid-state reaction synthesis method. The mixtures of BaS and HgS with stoichiometric ratio were heated to 800 °C in 20 h, kept there for 72 h, and then cooled to room temperature by switching off furnace.

$Ba_8Hg_4S_5Se_7$. The mixtures of BaS (0.034 g, 0.2 mmol), BaSe (0.303 g, 1.4 mmol), and HgS (0.186 g, 0.8 mmol) were loaded into quartz silica tubes (inner diameter: 10 mm, length: 20 mm), and the preparation process is similar to that for BHS. The sealed tubes were heated to 750 °C in 30 h, kept there for 48 h, and then slowly cooled to 300 °C with a rate of 3 K/h; finally, the furnace was switched off. Many bright red crystals were obtained in the tubes and are stable after months of observation.

Polycrystalline sample of BHSSe was prepared with the mixtures of BaS, BaSe, and HgS in the molar ratio of 1:7:4, which were kept at 700 °C for 72 h and then slowly cooled to room temperature.

Powder X-ray diffraction (XRD) analysis was measured at room temperature using an automated Bruker D2 X-ray diffractometer. A comparison between the calculated and experimental X-ray diffraction patterns is shown in Figure 1. In comparison, the experimental result (Figure 1a) is essentially in accordance with the calculated one from the single-crystal data of BHS. However, as for BHSSe, several extra peaks still exist after many solid-state reactions at different temperatures, which are corresponding to the byproducts of BHS and unreacted HgS. We think that both HgS and Se raw materials are easily sublimed at high temperature and separated from the reaction mixture; unfortunately, the sublimated material deviated from the stoichiometric ratio, and thus failed to obtain a single phase of BHSSe.

Structure Determination. Data collections were performed on a Bruker SMART APEX II 4K CCD diffractometer using Mo Kα radiation (λ = 0.710 73 Å) at 296(2) K. The crystal structure was solved by direct methods and refined using the SHELXTL program package.[33] The program XPREP was used for multiscan absorption corrections. The structure is checked with PLATON,[34a] and no other symmetry is found. As for BHSSe, during the refinement of its structure, the formula Ba_2HgSe_3 with R_1 = 6.05% was given by the first routine refinement, but the sites of Se2 and Se3 atoms have abnormal anisotropy parameter. The subsequent analysis of the element content in crystal with energy-dispersive X-ray (EDX) equipped Hitachi S-4800 SEM (Supporting Information, Figure S1 and Table S3) shows the approximate molar ratio of 8:4(3.88):5(4.72):7(7.28) for Ba, Hg, S, and Se. In comparison, the S and Se atoms were refined to occupy the same sites with a ratio of ~5:7 by the free occupancy refinement, and R_1 is converged to better value of 3.17%. Therefore, the formula

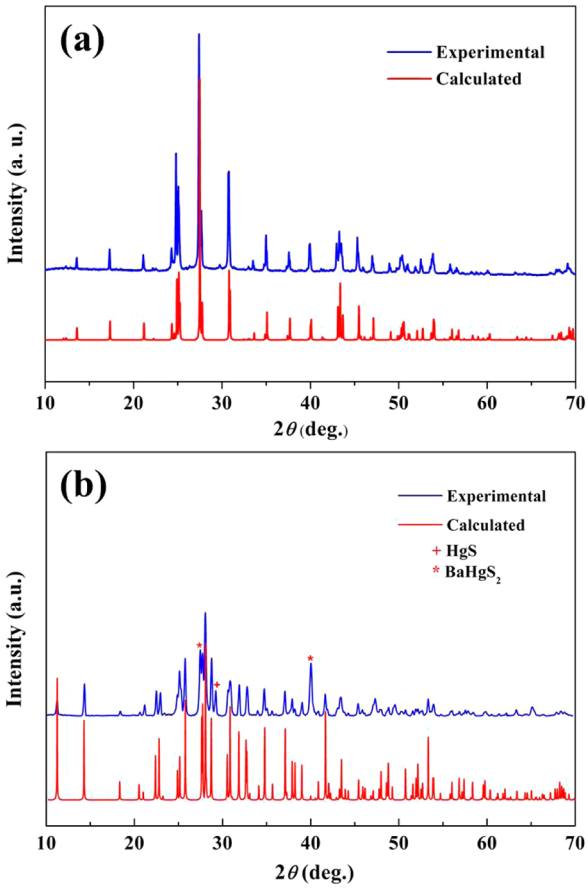

Figure 1. Powder XRD patterns of BHS (a) and BHSSe (b). (Red cross indicates impurity from HgS, asterisk indicates impurity from BHS).

$Ba_8Hg_4S_5Se_7$ was considered to be rational and agrees well with the test results ($Ba_8Hg_{3.88}S_{4.72}Se_{7.28}$) of EDX on this crystal. Crystal data and structure refinements of BHS and BHSSe are given in Table 1. Table S1a,b in the Supporting Information summarize the atomic coordinates and isotropic displacement parameters, and the related bond lengths and angles are shown in Table S2a,b in the Supporting Information.

UV−vis−near-IR Diffuse-Reflectance Spectroscopy. Diffuse reflectance spectra were measured with Shimadzu SolidSpec-3700DUV spectrophotometer at the wavelength range from 400 to 2500 nm.

Raman Spectroscopy. The Raman spectra of the crushed crystals were measured on a LABRAM HR Evolution spectrometer using 633 nm radiations. The crystals were put on a transparent glass slide and the measured area was chosen with a 50× objective lens. An integration time of 15 s was used to collect data, the experimental power was set to ~60 mW, and beam diameter of 35 μm was used.

Infrared Spectroscopy. IR spectroscopy was measured on a Shimadzu IRAffinity-1 Fourier transform infrared spectrometer. The data were collected in the wavenumber range from 400 to 4000 cm^{-1}. The samples are well-mixed with KBr powder at a mass ratio of 1:100 and pressed into thin disk that was used for IR spectrum test.

Thermal Analysis. The thermal analysis was measured on a simultaneous NETZSCH STA 449C thermal analyzer instrument. The crushed crystals were placed in Al_2O_3 crucibles, and the temperature was raised from 40 to 900 °C at 10 °C/min under N_2 atmosphere.

Second Harmonic Generation Measurement. The second harmonic generation (SHG) response test of BHS was measured on polycrystalline samples through the Kurtz and Perry method with a Cr:Tm:Ho:YAG Q-switch laser (2.09 μm, 3 Hz, 50 ns).[34b] Concerning

DOI: 10.1021/ic502939g
Inorg. Chem. 2015, 54, 2772−2779

Table 1. Crystal Data and Structure Refinement for BHSSe and BHS

empirical formula	$Ba_8Hg_4S_5Se_7$	$BaHgS_2$
formula weight	2614.10	402.05
temperature	296(2) K	296(2) K
crystal system	orthorhombic	orthorhombic
space group	*Pnma*	$Pmc2_1$
unit cell dimensions, Å	a = 9.051(9)	a = 4.217(5)
	b = 4.419(4)	b = 14.409(16)
	c = 17.550(17)	c = 7.335(8)
Z, V	1, 702.1(12) Å^3	4, 445.6(9) Å^3
density (calculated)	6.183 g/cm^3	5.993 g/cm^3
absorption coefficient	42.223 mm^{-1}	43.906 mm^{-1}
F (000)	1086	672
crystal size (mm^3)	0.061 × 0.063 × 0.141	0.052 × 0.078 × 0.139
limiting indices	$-11 \le h \le 11$	$-5 \le h \le 4$
	$-4 \le k \le 5$	$-15 \le k \le 18$
	$-20 \le l \le 22$	$-9 \le l \le 9$
reflections unique (R_{int})	0.0603	0.0413
completeness to θ = 27.61	99.8%	99.8%
goodness-of-fit on F^2	1.044	0.919
final R indices $[F_0^2 > 2\sigma(F_0^2)]^a$	R_1 = 0.0317	R_1 = 0.0318
	ωR_2 = 0.0621	ωR_2 = 0.0537
R indices (all data)^a	R_1 = 0.0461	R_1 = 0.0479
	ωR_2 = 0.0677	ωR_2 = 0.0581
extinction coefficient	0.000 80(12)	0.001 05(13)
largest diff. peak and hole	2.084 and −1.947 e·Å^{-3}	1.677 and −2.363 e·Å^{-3}

$^a R_1 = F_0 - F_c/F_0$ and $wR_2 = [w(F_0^2 - F_c^2)^2/wF_o^4]^{1/2}$ for $F_0^2 > 2\sigma(F_0^2)$

the phase-matching measurement, please see the previous report.[25a] Powder $AgGaS_2$ sample was used as the standard.

Theoretical Calculation. On the basis of ab initio calculations implemented in the CASTEP package, the density functional theory (DFT) was used to obtain electronic structures.[35] The Perdew–Burke–Ernzerhof (PBE) was used to calculate the exchange–correlation effects in the generalized gradient approximation (GGA).[36] The following orbital electrons were regarded as valence electrons, Ba: $5s^2\ 5p^6\ 6s^2$, Hg: $5d^{10}\ 6s^2$, S: $3s^2\ 3p^4$, Se: $4s^2\ 4p^4$. The energy cutoff of plane-wave basis set was 700.0 eV within normal-conserving pseudopotential (NCP),[37] and the Monkhorst–Pack scheme (3 × 6 × 2) for the Brillouin Zone was chosen.[38] As important parameters for NLO crystals, birefringence and SHG coefficients of BHS were also calculated.[39] Owing to the discontinuity of exchange correlation energy, the experimental value is usually larger than that of calculated band gap. Thus, scissors operators are always used to make the conduction bands (CB's) agree with the experimental values.[40]

The linear optical properties of the BHS crystal were obtained through the dielectric function formula $\varepsilon(\omega) = \varepsilon_1(\omega) + i\varepsilon_2(\omega)$. Among the formula, the imaginary part ε_2 can be calculated by the following equation:[41]

$$\varepsilon_2(q \to O_{\hat{u}}, h\omega) = \frac{2e^2\pi}{\Omega\varepsilon_o} \sum_{kcv} |\langle\varphi_k^c|u\cdot r|\varphi_k^v\rangle|^2\, \delta[E_k^c - E_k^v - E]$$

where e is the elementary charge, h is Planck's constant, u is the vector defining the polarization of the incident, r is the position operator, Ω is the volume of the unit cell, ε_o is the dielectric constant, $\varphi_k^{(c,v)}$ denote the momentum matrix element transition from the energy level c of the CB to the level v of the VB at the k point in the BZ. E_k^v and E_k^c are energies of occupied and empty electronic states, respectively. Then, the real part can be obtained by the Kramers–Kronig transformation. All the other optical parameters, including the absorption spectra, refractive index, and reflectivity, are also calculated from $\varepsilon_1(\omega)$ and $\varepsilon_2(\omega)$.[42]

By the length-gauge formalism, the SHG coefficients are achieved by the band wave functions.[43] The second-order nonlinear susceptibilities $\chi_{\alpha\beta\gamma}^{(2)}$ are reduced as[44]

$$\chi_{\alpha\beta\gamma}^{(2)} = \chi_{\alpha\beta\gamma}^{(2)}(\mathrm{VE}) + \chi_{\alpha\beta\gamma}^{(2)}(\mathrm{VH}) + \chi_{\alpha\beta\gamma}^{(2)}(\text{two-bands})$$

In this sum-over-states type formalism, the total SHG coefficient $\chi^{(2)}$ are divided into contribution from virtual-hole (VH), virtual-electron (VE) and two-bands (TB) processes. The contribution from two-bands process is so small that can be neglected. The formulas for calculating $\chi_{\alpha\beta\gamma}^{(2)}$ (VE), $\chi_{\alpha\beta\gamma}^{(2)}$ (VH), and $\chi_{\alpha\beta\gamma}^{(2)}$ (two band) are as follows

$$\chi_{\alpha\beta\gamma}^{(2)}(\mathrm{VE}) = \frac{e^3}{2\hbar m^3} \sum_{vv'c} \int \frac{d^3k}{4\pi^3} P(\alpha\beta\gamma)\mathrm{Im}[P_{vv'}^{\alpha} P_{cv}^{\beta} P_{cv}^{\gamma}] \times \left(\frac{1}{\omega_{cv}^3 \omega_{v'c}^2} + \frac{2}{\omega_{vc}^4 \omega_{cv'}}\right)$$

$$\chi_{\alpha\beta\gamma}^{(2)}(\mathrm{VH}) = \frac{e^3}{2\hbar m^3} \sum_{vcc'} \int \frac{d^3k}{4\pi^3} P(\alpha\beta\gamma)\mathrm{Im}[P_{cv}^{\alpha} P_{cc'}^{\beta} P_{c'v}^{\gamma}] \times \left(\frac{1}{\omega_{cv}^3 \omega_{vc'}^2} + \frac{2}{\omega_{vc}^4 \omega_{c'v}}\right)$$

$$\chi_{\alpha\beta\gamma}^{(2)}(\text{two-bands}) = \frac{e^3}{2\hbar m^3} \sum_{vc} \int \frac{d^3k}{4\pi^3} P(\alpha\beta\gamma) \times \frac{\mathrm{Im}[P_{vc}^{\alpha} P_{cv}^{\beta} (P_{vv}^{\gamma} - P_{cc}^{\gamma})]}{\omega_{vc}^5}$$

Here, α, β, γ are Cartesian components, v and v' denote valence bands, c and c' refer to conduction bands, and $P(\alpha\beta\gamma)$ denotes full permutation. The band energy difference and momentum matrix elements are denoted as $\hbar\omega_{ij}$ and P_{ij}^{α}, respectively. Furthermore, the theoretical methods were also applied with success to other NLO crystals in our previous study.[45]

DOI: 10.1021/ic502939g
Inorg. Chem. 2015, 54, 2772–2779

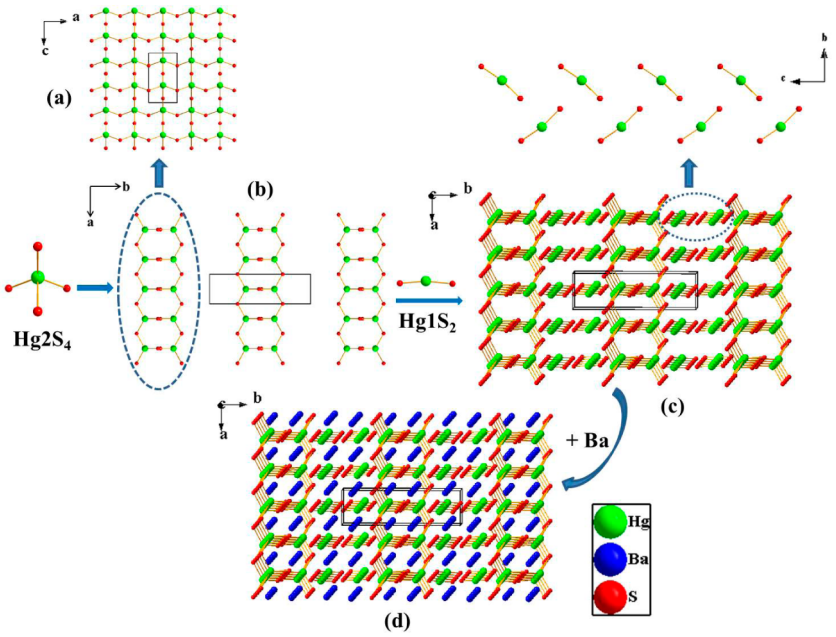

Figure 2. (a) A layer with corner-shared HgS_4 groups in the *ac* plane. (b) The HgS_4 layers stack along the *b*-axis. (c) Isolated $[HgS_2]$ units stack along the *c*-axis. (d) The 3D framework of BHS (all the Ba−S bonds are removed).

RESULTS AND DISCUSSION

Structure Description. $BaHgS_2$. BHS crystallizes in the orthorhombic space group $Pmc2_1$ with a = 4.217(5), b = 14.409(16), c =7.335(8) Å, and Z = 4. There are two unique Hg atoms, two Ba atoms, and four S atoms in its asymmetric unit.

The unique crystal structure of BHS is composed of $[HgS_4]$ tetrahedra units and isolated dumbbell-shaped $[HgS_2]$, forming a three-dimensional (3D) framework structure with charge-balanced Ba^{2+} cations (seen in Figure 2). In the structure, the Hg2 atoms are tetrahedrally coordinated to four S atoms forming $[HgS_4]$ units, and then the $[HgS_4]$ tetrahedra connect by corner sharing S atoms to make up a layered structure (Figure 2a), which stacks along the *c*-axis (Figure 2b). The Hg1 atoms are coordinated with two S atoms forming isolated $[HgS_2]$ units (Figure 2c). These layers are held together with charge-balanced Ba cations, giving rise to a 3D framework (Figure 2d). In addition, the S atoms exhibit three different types of coordination: (i) the S1 atoms have 6-fold coordination (4Ba and 2Hg); (ii) the S2 and S3 atoms have 5-fold coordination (4Ba and Hg), forming a square pyramid; (iii) the S4 atoms possess 4-fold coordination (2Ba and 2Hg), which are shown in Figure S2 in the Supporting Information. Note that the presence of isolated $[HgS_2]$ units in BHS is an important feature of this compound; in comparison with the structural characters of Ba_2HgS_3 and $BaCdS_2$,[31,46] both of them exhibit only $[HgS_4]$ and $[CdS_4]$ tetrahedra.

The interatomic distances of d(Ba−S) range from 3.171(6) to 3.324(2) Å, the mean distance for the Ba−S bond is 3.208 Å, and the S−Ba−S angles range from 71.2(2)° to 163.4(5)°. The Hg−S bond distances in the $[HgS_4]$ tetrahedron range from 2.443(5) to 3.028(5) Å, while the Hg−S bond distances in $[HgS_2]$ are 2.345(5) and 2.346(5) Å, respectively. The linear-like S−Hg−S angle is ∼166.78(17)°, which agrees well with other compounds containing $[HgS_2]$ units, such as Ba_2HgS_5 and $Cs_2Hg_3M_2S_8$ (M = Ge, Sn).[32,47] The calculated bond valence sums (BVS's) are 1.966−2.158, 1.864−1.953, and 1.604−2.214 for Ba^{2+}, Hg^{2+}, and S^{2-}, respectively.

$Ba_8Hg_4S_5Se_7$. BHSSe crystallizes in the orthorhombic space group *Pnma* with a = 9.051(9) Å, b = 4.419(4) Å, and c = 17.550(17) Å. In the structure of BHSSe, the Hg atoms are coordinated with two selenium and two S/Se atoms forming $[HgSe_2(S/Se)_2]$ units, and then by corner-sharing a Se atom the $[HgSe_2(S/Se)_2]$ tetrahedra form infinite isolated chains, which are parallel to the *b* axis (Figure 3a). These layers are held together with Ba cations, giving rise to a 3D framework (Figure 3c). The charge density was further used to understand the bonding interactions (Figure 4). As a result, the bonding interaction of Hg−Se and Hg−S/Se are covalent, since there has considerable charge density between the Hg atoms, and between Se and S in the $[HgSe_2(S/Se)_2]$ subunits. In addition, as for Ba sites, there have ionic interactions with the existence of spherically distributed charges.

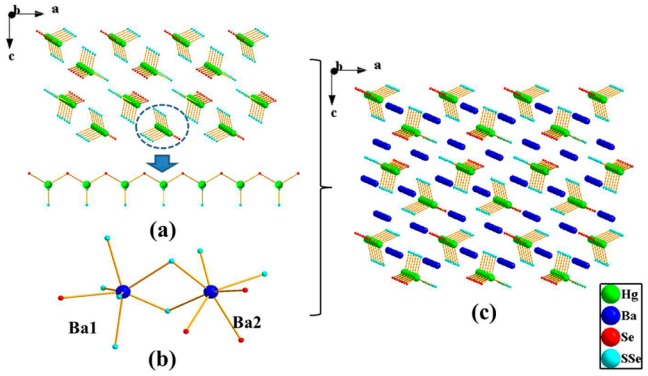

Figure 3. (a) The infinite $_\infty[HgSe_2(S/Se)_2]_n$ chains are shown after 30° rotation along the *b* axis. (b) The coordinated environments of the Ba atoms in BHSSe. (c) The 3D framework of BHSSe with Ba−Se and Ba−S/Se bonds omitted for clarity viewing after 30° rotation along *b* axis.

DOI: 10.1021/ic502939g
Inorg. Chem. 2015, 54, 2772−2779

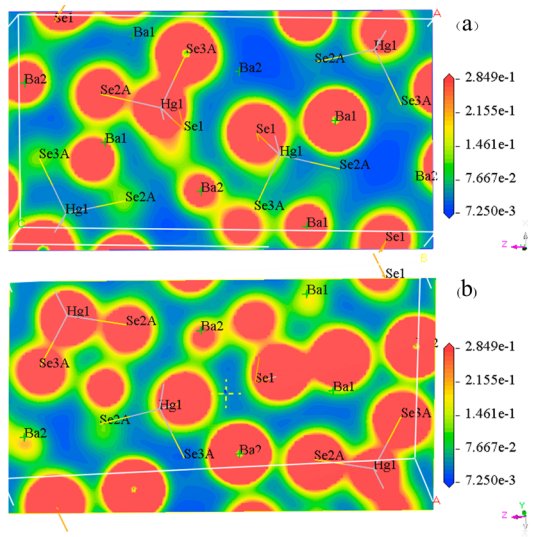

Figure 4. Calculated electron density of BHSSe.

The Hg atom is connected with two Se atoms and two S/Se atoms to form a $[HgSe_2(S/Se)_2]$ tetrahedron with distances of Hg−Se (2.649(2) Å) and Hg−S/Se range from 2.582(3)−2.590(3) Å, which is close to the average Hg-Q (Q=S, Se) bond distances of other compounds, such as $K_2Hg_3S_4$ (2.57(1) Å), $K_2Hg_3Se_4$ (2.66(1) Å), and $Cs_2Hg_3Se_4$ (2.68(8) Å). The Ba1 atoms are coordinated by three Se and four S/Se atoms to make up the distortional $[Ba1Se_3(S/Se)_4]$ polyhedron with the distance of Ba−Se ranging from 3.302(2)−3.444(3) Å and Ba−S/Se ranging from 3.143(3)−3.229(4) Å, and the Ba2 atoms are surrounded by one Se and six S/Se atoms to make up the $[Ba2Se(S/Se)_6]$ polyhedron with the distance of Ba−Se (3.382(4) Å) and Ba−S/Se range from 3.262(3)−3.362(3) Å, which are close to those in other compounds, such as $BaGa_4Se_7$ (3.429(2)−3.861(2) Å), Ba_2CdSe_3 (3.216(3)−3.521(3) Å) and $Ba_2In_2Se_5$ (3.212(2)−3.873(2) Å).[48] The calculated BVS are 1.884−2.32, 2.37, 2.35 and 2.061−2.164 for Ba^{2+}, Hg^{2+}, Se^{2-} and $(S/Se)^{2-}$, respectively.

Experimental Band Gaps. As seen from the measured diffuse-reflectance spectra, the band gaps are obtained to be 1.93 and 1.98 eV (Figure 5) by a straightforward extrapolation method, and the corresponding absorption edges are 642 and 626 nm for BHS and BHSSe, respectively.[49] Their band gaps are slightly larger than that of classical $AgGaSe_2$ compound (1.8 eV),[50] which shows that the titled compounds may have high laser induced damage threshold for practical application. The IR transmission spectra of BHS and BHSSe are shown in Figure S3 in the Supporting Information. Both of the title compounds exhibit a wide IR transmission up to 20 μm, which indicates that the title compounds have potential application as effective IR materials.

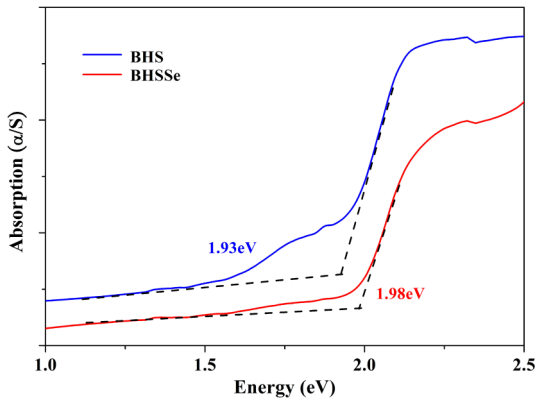

Figure 5. Experimental band gaps of BHS and BHSSe.

Raman Spectroscopy. As seen from the Raman spectra (Figure S4 in the Supporting Information), two broad peaks of BHS (266 and 310 cm^{-1}) and BHSSe (267 and 311 cm^{-1}) are shown, which can be assigned to mercury−sulfur or mercury−selenium vibrations. And the Ba−S/Se or Ba−S vibrations are corresponding to the peaks below 200 cm^{-1}.

Thermal Analysis. $BaHgS_2$. The thermogravimetric (TG) and differential scanning calorimetry (DSC) curves are shown in Figure S5a in the Supporting Information, where it can be seen that BHS is thermally stable up to 450 °C and starts to decompose into easily sublimated materials (HgS) above 450 °C.

$$BaHgS_2 \rightarrow BaS + HgS\uparrow$$

According to the above equation, the weight loss of sublimated HgS is calculated to be ∼58%, which agrees well with the measured result from the TG curve. In addition, there has one endothermic peak at ∼642 °C, which is corresponding to the sublimation of HgS.

$Ba_8Hg_4S_5Se_7$. The TG and DSC curves are depicted in Figure S5b in the Supporting Information. From the figure, BHSSe is thermally stable at ∼400 °C and has two obviously endothermic peaks located at 650 and 752 °C, respectively. While the measured temperature is higher than 400 °C, the samples start to decompose into easily sublimated materials, such as HgS and Se, giving rise to the weight loss of sample. Therefore, two endothermic peaks are corresponding to the sublimation of HgS (650 °C) and Se (752 °C) from the DSC curve, respectively.

Second Harmonic Generation Measurement. The powder SHG property of the BHS compound was measured. The particle size versus SHG intensity of BHS indicates a nonphase matching behavior at 2.09 μm (Figure S6 in the Supporting Information). Remarkably, as seen from Figure 6, BHS has ∼6.5 times that of standard $AgGaS_2$ at the 38−88 μm particle size. Therefore, BHS may have good potential as an efficient NLO IR material.

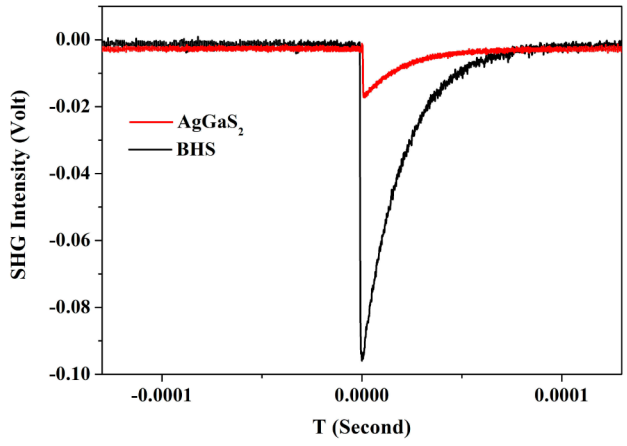

Figure 6. Relative intensity of SHG signals for BHS vs $AgGaS_2$ with the 38−88 μm particle size.

DOI: 10.1021/ic502939g
Inorg. Chem. 2015, 54, 2772−2779

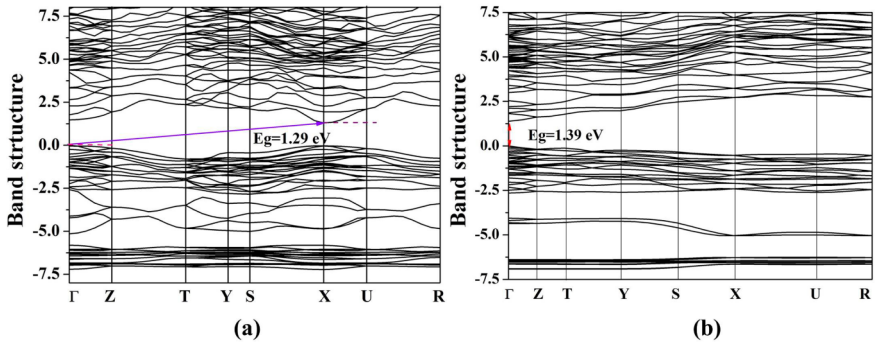

Figure 7. Band structures of BHS (a) and BHSSe (b).

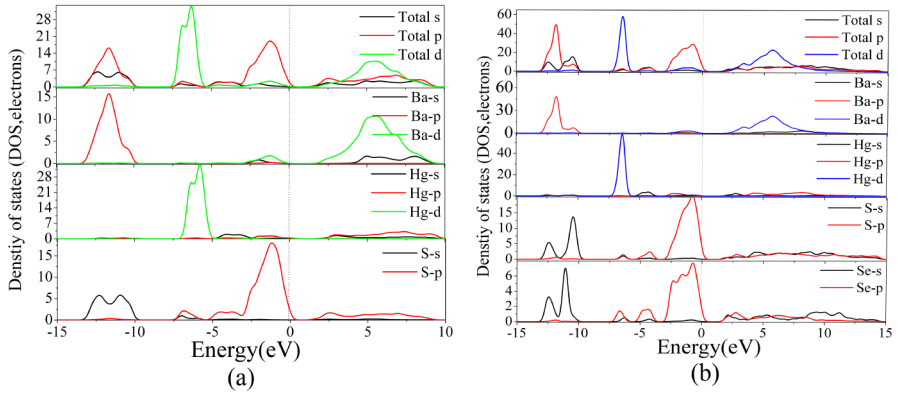

Figure 8. Total and partial densities of states (PDOS and TDOS) plots of BHS (a) and BHSSe (b).

Theoretical Studies. To realize further investigations on the structure and optical properties of BHS and BHSSe, theoretical calculations were used by DFT methods. Results of the band structure calculations (Figure 7) indicate that BHS is an indirect band gap, while BHSSe is a direct band gap, and the calculated values of BHS and BHSSe are 1.29 and 1.39 eV, respectively, smaller than the experimental values (1.93 and 1.98 eV, Figure 5). To ensure the accuary of calculated optical parameters, the scissors of 0.64 and 0.59 eV are used in the calculations of optical parameters for BHS and BHSSe, respectively.

Figure 8 shows the total and partial densities of states (PDOS and TDOS) of title compounds. We focus our attention on the vicinity of Fermi level (FL), which counts for most of the bonding character and is bound with the optical parameters. For BHS (Figure 8a), the valence band (VB) near the FL can be divided into four regions: from −13.5 to −10.0 eV, S 3s states overlap completely with Ba 5p, showing strong Ba−S covalent interactions. And the bands in region (−7.5 to −5.0 eV) mainly come from Hg 5d and S 3p states, which shows some contributions to the Hg−S bonds. The upper part of VB from −5 eV to FL shows some of hybridizations between Ba 5s, S 3p and Hg 5s, 5p orbitals, revealing a few of chemical bonds between the Ba−S and Hg−S, but the top VB maximum is dominated by S 3p orbitals. In addition, for the CB bottom (1.29 to 10 eV), it is dominated with the orbitals of all atoms, and the S 3p orbitals determine the CB minimum of the BHS crystal.

Figure 8b gives the PDOS projected onto the component atoms of the BHSSe crystal, in which a number of electronic features can be seen: (i) The region between −13.5 and −10 eV mainly consists of 3s and 4s orbitals of sulfur and selenium atoms, and 5p orbitals of the barium atoms. (ii) The VB (−7.5 to −5.5 eV) is mainly from the contributions of S 3p and Se 4p states with some of Hg 5d orbitals, and the bands in region (−5.5 to −3.0 eV) mainly come from Hg 6s and S 3p, and Se 4p states, which have some contributions to the Hg−S and Hg−Se bonds. Near the top of the VB (from −3.0 to FL), there is obvious hybridization between the orbitals of S and Se atoms. (iii) From the 1.39 to 15 eV of CB, which is originated from the orbitals of all atoms, and the S 3p and Se 4p orbitals dominate the CB minimum of the BHSSe crystal. Therefore, the calculated PDOS shows that both the upper part of the VB and the bottom area of the CB are mainly dominated by 3p orbitals of sulfur atoms and 4p orbitals of selenium.

Optical Properties. On the basis of the electronic structures, the imaginary part ε_2 and real part ε_1 can be determined (Figure S7 in the Supporting Information), and the refractive indices of BHS were also calculated.[42] The calculated refractive indices show strong anisotropy: $n^x \approx n^y > n^z$ for BHS and the curve of birefringence (Δn) versus wavelength is shown in Figure 9. It can be seen that the birefringence Δn is ∼0.07 with the wavelength ∼1 μm. Moreover, we also obtained the SHG coefficients of BHS as follows: d_{31} = 5.2, d_{32} = −16.7 and d_{33} = −59.7 pm/V. The calculated maximum result is consistent with the test observation that BHS exhibits an SHG response that is 5−6 times that of $AgGaS_2$ (d_{36} = 11 pm/V), which indicates that BHS is a potential NLO IR material for practical application.

■ CONCLUSIONS

In summary, we have synthesized two mid-IR transparency compounds: acentric BHS and centric BHSSe. For centric BHSSe, the Hg atoms are connected with two selenium and

DOI: 10.1021/ic502939g
Inorg. Chem. 2015, 54, 2772−2779

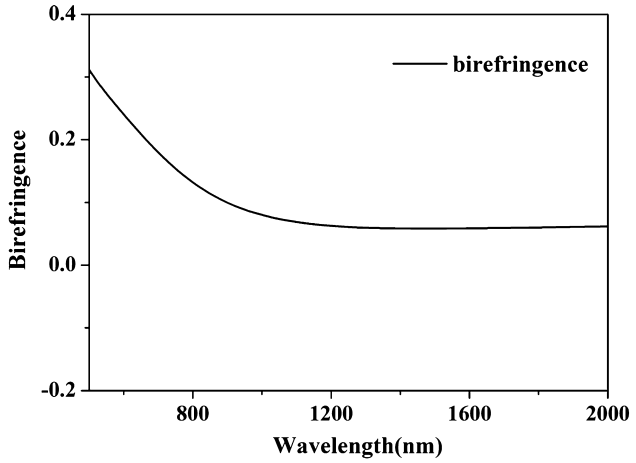

Figure 9. Calculated birefringence of BHS.

two S/Se atoms forming $[HgSe_2(S/Se)_2]$ units. The acentric BHS has two different coordination patterns of $[HgS_4]$ tetrahedra and isolated dumbbell-shaped $[HgS_2]$ units. The Raman spectroscopy and thermal analysis of the title compounds show that they have wide IR transimission range and good thermal stability. In addition, the band gaps of BHS and BHSSe are 1.93 and 1.98 eV, respectively, according to the diffuse-reflectance measurement. The calculated DOS shows that the energy band gaps are mainly determined by 3p orbitals of sulfur atoms and 4p orbitals of selenium for BHSSe or 3p orbitals of sulfur atoms for BHS, respectively. Remarkably, the powder BHS sample exhibits a good SHG response, ~6.5 times that of the standard $AgGaS_2$ sample at 2.09 μm. The calculated SHG tensor elements of acentric BHS are d_{31} = 5.2, d_{32} = −16.7, and d_{33} = −59.7 pm/V, which agree with the experimental data. Therefore, BHS may have good potential as an efficient NLO IR material.

■ ASSOCIATED CONTENT

Supporting Information

CIF files; atomic coordinates and isotropic displacement parameters, and selected bond distances and angles tables for BHS and BHSSe; EDX spectrum and data for BHSSe; Raman and IR spectra, TG and DSC curves of BHS and BHSSe; calculated dielectric function of BHS; particle size versus SHG intensity for BHS. This material is available free of charge via the Internet at http://pubs.acs.org.

■ AUTHOR INFORMATION

Corresponding Author

*E-mail: slpan@ms.xjb.ac.cn. Phone: (+86)991-3674558. Fax: (+86)991-3838957.

Notes

The authors declare no competing financial interest.

■ ACKNOWLEDGMENTS

This work was supported by the Xinjiang Program of Cultivation of Young Innovative Technical Talents (Grant No. 2014731029), the Western Light Foundation of Chinese Academy of Sciences (CAS, Grant No. XBBS201318), the National Natural Science Foundation of China (Grant Nos. 51402352 and 51425206), the Funds for Creative Cross & Cooperation Teams of CAS, Xinjiang International Science & Technology Cooperation Program (20146001).

■ REFERENCES

(1) (a) Duarte, F. J. *Tunable Laser Applications,* 2nd ed.; CRC Press: Boca Raton, FL, 2008; Chapters 2, 9, and 12. (b) Byer, R. L. *Science* **1988**, *239*, 742−747. (c) Keller, U. *Nature* **2003**, *424*, 831−838. (d) Demtröder, W. *Laser Spectroscopy,* 3rd ed.; Springer, Berlin, Germany, 2009.

(2) (a) Geusic, J. E.; Marcos, H. M.; Van-Uitert, L. G. *Appl. Phys. Lett.* **1964**, *4*, 182−184. (b) Lacovara, P.; Choi, H. K.; Wang, C. A.; Aggarwal, R. L.; Fan, T. Y. *Opt. Lett.* **1991**, *16*, 1089−1091. (c) Krupke, W. F. *IEEE J. Sel. Top. Quantum Electron.* **2000**, *6*, 1287−1296.

(3) (a) Franken, P. A.; Hill, A. E.; Peters, C. W.; Weinrich, G. *Phys. Rev. Lett.* **1961**, *7*, 118−119. (b) Burland, D. M.; Miller, R. D.; Walsh, C. A. *Chem. Rev.* **1994**, *94*, 31−75.

(4) (a) Chen, C. T.; Wu, B. C.; Jiang, A. D.; You, G. M. *Sci. Sin., Ser. B (Engl. Ed.)* **1985**, *28*, 235−243. (b) Chen, C. T.; Wu, Y. C.; Jiang, A. D.; Wu, B. C.; You, G. M.; Li, R. K.; Lin, S. J. *J. Opt. Soc. Am. B* **1989**, *6*, 616−621. (c) Wu, Y. C.; Sasaki, T.; Nakai, S.; Yokotani, A.; Tang, H.; Chen, C. T. *Appl. Phys. Lett.* **1993**, *62*, 2614−2615. (d) Mori, Y.; Kuroda, I.; Nakajima, S.; Sasaki, T.; Nakai, S. *Appl. Phys. Lett.* **1995**, *67*, 1818−1820.

(5) (a) Chen, C. T.; Wang, Y.; Wu, B. C.; Zeng, W.; Yu, L. *Nature* **1995**, *373*, 322−324. (b) Mei, L.; Wang, Y.; Chen, C. T.; Wu, B. C. *J. Appl. Phys.* **1993**, *74*, 7014−7016. (c) Lu, J. H.; Wang, G. L.; Xu, Z. Y.; Chen, C. T.; Wang, J. Y.; Zhang, C. Q.; Liu, Y. G. *Chin. Phys. Lett.* **2002**, *19*, 680−681.

(6) (a) Hu, Z. G.; Yoshimura, M.; Muramatsu, K.; Mori, Y.; Sasaki, T. *Jpn. J. Appl. Phys.* **2002**, *41*, 1131−1133. (b) Becker, P. *Adv. Mater.* **1998**, *10*, 979−992.

(7) (a) Eckardt, R. C.; Masuda, H.; Fan, Y. X.; Byer, R. L. *IEEE J. Quantum Electron.* **1990**, *26*, 922−933. (b) Driscoll, T. A.; Hoffman, H. J.; Stone, R. E.; Perkins, P. E. *J. Opt. Soc. Am. B* **1986**, *3*, 683−686. (c) Boyd, G. D.; Miller, R. C.; Nassau, K.; Bond, W. L.; Savage, A. *Appl. Phys. Lett.* **1964**, *5*, 234−236.

(8) Nikogosyan, D. N. *Nonlinear Optical Crystals: A Complete Survey,* 1st ed.; Springer: New York, 2005.

(9) (a) Chemla, D. S.; Kupecek, P. J.; Robertson, D. S.; Smith, R. C. *Opt. Commun.* **1971**, *3*, 29−31. (b) Boyd, G. D.; Kasper, H. M.; McFee, J. H.; Storz, F. G. *IEEE J. Quantum Electron.* **1972**, *8*, 900−908. (c) Boyd, G. D.; Buehler, E.; Storz, F. G. *Appl. Phys. Lett.* **1971**, *18*, 301−304. (d) Fossier, S.; Salaun, S.; Mangin, J.; Bidault, O.; Thenot, I.; Zondy, J. J.; Chen, W. D.; Rotermund, F.; Petrov, V.; Petrov, P.; Henningsen, J.; Yelisseyev, A.; Isaenko, L.; Lobanov, S.; Balachninaite, O.; Slekys, G.; Sirutkaitis, V. *J. Opt. Soc. Am. B* **2004**, *21*, 1981−2007.

(10) (a) Ok, K. M.; Halasyamani, P. S. *Chem. Soc. Rev.* **2006**, *35*, 710−717. (b) Marvel, M. R.; Lesage, J.; Baek, J.; Halasyamani, P. S.; Stern, C. L.; Poeppelmeier, K. R. *J. Am. Chem. Soc.* **2007**, *129*, 13963−13969. (c) Bader, R. F. W. *Mol. Phys.* **1960**, *3*, 137−140. (d) Bader, R. F. W. *Can. J. Chem.* **1962**, *40*, 1164−1175. (e) Pearson, R. G. *J. Am. Chem. Soc.* **1969**, *91*, 4947−4955. (f) Wheeler, R. A.; Whangbo, M. H.; Hughbanks, T.; Hoffmann, R.; Burdett, J. K.; Albright, T. A. *J. Am. Chem. Soc.* **1986**, *108*, 2222−2228.

(11) (a) Porter, Y.; Halasyamani, P. S. *J. Solid State Chem.* **2003**, *174*, 441−449. (b) Ra, H. S.; Ok, K. M.; Halasyamani, P. S. *J. Am. Chem. Soc.* **2003**, *125*, 7764−7769. (c) Ok, K. M.; Halasyamani, P. S. *Angew. Chem., Int. Ed.* **2004**, *43*, 5489−5491. (d) Chang, H. Y. S.; Kim, H.; Halasyamani, P. S.; Ok, K. M. *J. Am. Chem. Soc.* **2009**, *131*, 2426−2427. (e) Yeon, J.; Kim, S.; Nguyen, S. D.; Lee, H.; Halasyamani, P. S. *Inorg. Chem.* **2012**, *51*, 2662−2668. (f) Kim, S. H.; Yeon, J.; Halasyamani, P. S. *Chem. Mater.* **2009**, *21*, 5335−5342. (g) Lee, D. W.; Ok, K. M. *Inorg. Chem.* **2014**, *53*, 10642−10648. (h) Song, S. Y.; Lee, D. W.; Ok, K. M. *Inorg. Chem.* **2014**, *53*, 7040−7046. (i) Bae, S. W.; Kim, C. Y.; Lee, D. W.; Ok, K. M. *Inorg. Chem.* **2014**, *53*, 11328−11334.

(12) (a) Rong, C.; Yu, Z. W.; Wang, Q.; Zheng, S. T.; Pan, C. Y.; Deng, F.; Yang, G. Y. *Inorg. Chem.* **2009**, *48*, 3650−3659. (b) Zhou, J.; Zheng, S. T.; Zhang, M. Y.; Liu, G. Z.; Yang, G. Y. *CrystEngComm* **2009**, *11*, 2597−2600. (c) Cheng, L.; Wei, Q.; Wu, H. Q.; Zhou, L. J.; Yang, G. Y. *Chem.—Eur. J.* **2013**, *19*, 17662−17667. (d) Wang, G. M.; Sun, Y. Q.; Yang, G. Y. *Cryst. Growth Des.* **2005**, *5*, 313−317.

DOI: 10.1021/ic502939g
Inorg. Chem. 2015, 54, 2772−2779

(13) (a) Zou, G. H.; Huang, L.; Ye, N.; Lin, C. S.; Cheng, W. D.; Huang, H. *J. Am. Chem. Soc.* **2013**, *135*, 18560−18566. (b) Zou, G. H.; Ye, N.; Huang, L.; Lin, X. S. *J. Am. Chem. Soc.* **2011**, *133*, 20001−20007.
(14) (a) Zhang, J. H.; Hu, C. L.; Xu, X.; Kong, F.; Mao, J. G. *Inorg. Chem.* **2011**, *50*, 1973−1782. (b) Kong, F.; Jiang, H. L.; Hu, T.; Mao, J. G. *Inorg. Chem.* **2008**, *47*, 10611−10617. (c) Hao, Y. C.; Hu, C. L.; Xu, X.; Kong, F.; Mao, J. G. *Inorg. Chem.* **2013**, *52*, 13644−13650.
(15) (a) Pilz, T.; Jansen, M. *Z. Anorg. Allg. Chem.* **2011**, *637*, 1−6. (b) Cakmak, G.; Nuss, J.; Jansen, M. *Z. Anorg. Allg. Chem.* **2009**, *635*, 631−636. (c) Pilz, T.; Nuss, H.; Jansen, M. *J. Solid State Chem.* **2012**, *186*, 104−108.
(16) (a) Li, F.; Hou, X. L.; Pan, S. L.; Wang, X. A. *Chem. Mater.* **2009**, *21*, 2846−2850. (b) Wu, H. P.; Pan, S. L.; Poeppelmeier, K. R.; Li, H. Y.; Jia, D. Z.; Chen, Z. H.; Fan, X. Y.; Yang, Y.; Rondinelli, J. M.; Luo, H. S. *J. Am. Chem. Soc.* **2011**, *133*, 7786−7790. (c) Yu, H. W.; Pan, S. L.; Wu, H. P.; Zhao, W. W.; Zhang, F. F.; Li, H. Y.; Yang, Z. H. *J. Mater. Chem.* **2012**, *22*, 2105−2110. (d) Yu, H. W.; Wu, H. P.; Pan, S. L.; Yang, Z. H.; Su, X.; Zhang, F. F. *J. Mater. Chem.* **2012**, *22*, 9665−9670. (e) Wu, H. P.; Yu, H. W.; Pan, S. L.; Huang, Z. J.; Yang, Z. H.; Su, X.; Poeppelmeier, K. R. *Angew. Chem., Int. Ed.* **2013**, *52*, 3406−3410. (f) Yu, H. W.; Wu, H. P.; Pan, S. L.; Yang, Z. H.; Hou, X. L.; Su, X.; Jing, Q.; Poeppelmeier, K. R.; Rondinelli, J. M. *J. Am. Chem. Soc.* **2014**, *136*, 1264−1267.
(17) (a) Yang, Y.; Pan, S. L.; Hou, X. L.; Wang, C.; Poeppelmeier, K. R.; Chen, Z. H.; Wu, H. P.; Zhou, Z. X. *J. Mater. Chem.* **2011**, *21*, 2890−2894. (b) Yang, Y.; Pan, S. L.; Li, H. L.; Han, J.; Chen, Z. H.; Zhao, W. W.; Zhou, Z. X. *Inorg. Chem.* **2011**, *50*, 2415−2419. (c) Pan, S. L.; Wu, Y. C.; Fu, P. Z.; Zhang, G. C.; Li, Z. H.; Du, C. X.; Chen, C. T. *Chem. Mater.* **2003**, *15*, 2218−2221.
(18) (a) Huang, H. W.; Yao, J. Y.; Lin, Z. S.; Wang, X. Y.; He, R.; Yao, W. J.; Zhai, N. X.; Chen, C. T. *Chem. Mater.* **2011**, *23*, 5457−5463. (b) Huang, H. W.; Yao, J. Y.; Lin, Z. S.; Wang, X. Y.; He, R.; Yao, W. J.; Zhai, N. X.; Chen, C. T. *Angew. Chem., Int. Ed.* **2011**, *50*, 9141−9144.
(19) (a) Yao, W. J.; Huang, H. W.; Yao, J. Y.; Xu, T.; Jiang, X. X.; Lin, Z. S.; Chen, C. T. *Inorg. Chem.* **2013**, *52*, 6136−6141. (b) Zhao, S. G.; Zhang, J.; Zhang, S. Q.; Sun, Z. H.; Lin, Z. S.; Wu, Y. C.; Hong, M. C.; Luo, J. H. *Inorg. Chem.* **2014**, *53*, 2521−2527.
(20) (a) Xia, M. J.; Li, R. K. *J. Solid State Chem.* **2013**, *201*, 288−292. (b) Chung, I.; Kanatzidis, M. G. *Chem. Mater.* **2014**, *26*, 849−869.
(21) (a) Chung, I.; Malliakas, C. D.; Jang, J. I.; Canlas, C. G.; Weliky, D. P.; Kanatzidis, M. G. *J. Am. Chem. Soc.* **2007**, *129*, 14996−15006. (b) Chung, I.; Jang, J. I.; Malliakas, C. D.; Ketterson, J. B.; Kanatzidis, M. G. *J. Am. Chem. Soc.* **2010**, *132*, 384−389. (c) Chung, I.; Kim, M. G.; Jang, J. I.; He, J.; Ketterson, J. B.; Kanatzidis, M. G. *Angew. Chem., Int. Ed.* **2011**, *50*, 10867−10870.
(22) (a) Bera, T. K.; Jang, J. I.; Song, J. H.; Malliakas, C. D.; Freeman, A. J.; Ketterson, J. B.; Kanatzidis, M. G. *J. Am. Chem. Soc.* **2010**, *132*, 3484−3495. (b) Bera, T. K.; Song, J. H.; Freeman, A. J.; Jang, J. I.; Ketterson, J. B.; Kanatzidis, M. G. *Angew. Chem., Int. Ed.* **2008**, *47*, 7828−7832.
(23) (a) Kanatzidis, M. G.; Huang, S. P. *Inorg. Chem.* **1989**, *28*, 4667−4669. (b) Bera, T. K.; Jang, J. I.; Ketterson, J. B.; Kanatzidis, M. G. *J. Am. Chem. Soc.* **2009**, *131*, 75−77. (c) Chung, I.; Song, J. H.; Jang, J. I.; Freeman, A. J.; Ketterson, J. B.; Kanatzidis, M. G. *J. Am. Chem. Soc.* **2009**, *131*, 2647−2656.
(24) (a) Chen, M. C.; Wu, L. M.; Lin, H.; Zhou, L. J.; Chen, L. *J. Am. Chem. Soc.* **2012**, *134*, 6058−6060. (b) Chen, Y. K.; Chen, M. C.; Zhou, L. J.; Chen, L.; Wu, L. M. *Inorg. Chem.* **2013**, *52*, 8334−8341.
(25) (a) Lin, H.; Zhou, L. J.; Chen, L. *Chem. Mater.* **2012**, *24*, 3406−3414. (b) Mei, D. J.; Yin, W. L.; Feng, K.; Lin, Z. S.; Bai, L.; Yao, J. Y.; Wu, Y. C. *Inorg. Chem.* **2012**, *51*, 1035−1040. (c) Lekse, J. W.; Moreau, M. A.; McNerny, K. L.; Yeon, J.; Halasyamani, P. S.; Aitken, J. A. *Inorg. Chem.* **2009**, *48*, 7516−7518.
(26) (a) Li, P.; Li, L. H.; Chen, L.; Wu, L. M. *J. Solid State Chem.* **2010**, *183*, 444−450. (b) Chen, M. C.; Li, P.; Zhou, L. J.; Li, L. H.; Chen, L. *Inorg. Chem.* **2011**, *50*, 12402−12404.
(27) (a) Kanatzidis, M. G.; Park, Y. *Chem. Mater.* **1990**, *2*, 99−101. (b) Kanatzidis, M. G.; Sutorik, A. C. *Prog. Inorg. Chem.* **1995**, *43*, 151−265. (c) Axtell, E. A.; Park, Y.; Chondroudis, K.; Kanatzidis, M. G. *J. Am. Chem. Soc.* **1998**, *120*, 124−136.
(28) (a) Atuchin, V. V.; Kesler, V. G.; Ursaki, V. V.; Tezlevan, V. E. *Solid State Commun.* **2006**, *138*, 250−254. (b) Rotermund, F.; Petrov, V.; Noack, F. *Opt. Commun.* **2000**, *185*, 177−183. (c) Liao, J. H.; Marking, G. M.; Hsu, K. F.; Matsushita, Y.; Ewbank, M. D.; Borwick, R.; Cunningham, P.; Rosker, M. J.; Kanatzidis, M. G. *J. Am. Chem. Soc.* **2003**, *125*, 9484−9493.
(29) Bai, L.; Lin, Z. S.; Wang, Z. Z.; Chen, C. T. *J. Appl. Phys.* **2008**, *103*, 083111−1.
(30) Rad, H. D.; Hoppe, R. Z. *Anorg. Allg. Chem.* **1981**, *483*, 18−25.
(31) Rad, H. D.; Hoppe, R. Z. *Anorg. Allg. Chem.* **1981**, *483*, 7−17.
(32) Islam, S. M.; Im, J.; Freeman, A. J.; Kanatzidis, M. G. *Inorg. Chem.* **2014**, *53*, 4698−4704.
(33) Sheldrick, G. M. *SHELXTL,* version 6.14; Bruker Analytical X-ray Instruments, Inc.: Madison, WI, 2008.
(34) (a) Spek, A. L. *J. Appl. Crystallogr.* **2003**, *36*, 7−13. (b) Kurtz, S. K.; Perry, T. T. *J. Appl. Phys.* **1968**, *39*, 3798−3813.
(35) Clark, S. J.; Segall, M. D.; Pickard, C. J.; Hasnip, P. J.; Probert, M. J.; Refson, K.; Payne, M. C. *Z. Kristallogr.* **2005**, *220*, 567−570.
(36) Kohn, W.; Sham, L. J. *Phys. Rev.* **1965**, *140*, 1133−1138.
(37) Perdew, J. P.; Burke, K.; Ernzerhof, M. *Phys. Rev. Lett.* **1996**, *77*, 3865−3868.
(38) (a) Monkhorst, H. J.; Pack, J. D. *Phys. Rev. B* **1976**, *13*, 5188−5192. (b) Perdew, J. P.; Wang, Y. *Phys. Rev. B* **1992**, *45*, 13244−13249.
(39) Chen, C. T.; Lin, Z. S.; Wang, Z. Z. *Appl. Phys. B: Laser Opt.* **2005**, *80*, 1−25.
(40) (a) Godby, R. W.; Schluter, M.; Sham, L. J. *Phys. Rev. B* **1988**, *37*, 10159−10175. (b) Wang, C. S.; Klein, B. M. *Phys. Rev. B* **1981**, *24*, 3417−3429.
(41) Palik, E. D. *Handbook of Optical Constants of Solids;* Academic Press: New York, 1985.
(42) Wooten, F. *Optical Properties of Solid;* Academic: New York, 1972.
(43) Aversa, C.; Sipe, J. E. *Phys. Rev. B* **1995**, *52*, 14636−14645.
(44) Lin, J.; Lee, M. H.; Liu, Z. P.; Chen, C.; Pickard, C. J. *Phys. Rev. B* **1999**, *60*, 13380−13389.
(45) (a) Su, X.; Wang, Y.; Yang, Z. H.; Huang, X. C.; Pan, S. L.; Li, F.; Lee, M. H. *J. Phys. Chem. C* **2013**, *117*, 14149−14157. (b) Zhang, B. B.; Yang, Z. H.; Yang, Y.; Lee, M. H.; Pan, S. L.; Jing, Q.; Su, X. *J. Mater. Chem. C* **2014**, *2*, 4133−4141. (c) Jing, Q.; Dong, X. Y.; Yang, Z. H.; Pan, S. L.; Zhang, B. B.; Huang, X. C.; Chen, M. W. *J. Solid State Chem.* **2014**, *219*, 138−142.
(46) Iglesias, J. E.; Pachalis, K. E.; Steinfink, H. *J. Solid State Chem.* **1974**, *9*, 6−14.
(47) Marking, G. A.; Hanko, J. A.; Kanatzidis, M. G. *Chem. Mater.* **1998**, *10*, 1191−1199.
(48) (a) Eisenmann, B.; Hofmann, A. *Z. Anorg. Allg. Chem.* **1990**, *580*, 151−159. (b) Schevciw, O.; White, W. B. *Mater. Res. Bull.* **1983**, *18*, 1059−1068. (c) Yao, J. Y.; Mei, D. J.; Bai, L.; Lin, Z. S.; Yin, W. L.; Fu, P. Z.; Wu, Y. C. *Inorg. Chem.* **2010**, *49*, 9212−9216.
(49) Chen, S. Y.; Gong, X. G.; Wei, S. H. *Phys. Rev. B* **2007**, *75*, 205209 1−9.
(50) Byer, R. L.; Choy, M. M.; Herbst, R. L.; Chemla, D. S.; Feigelson, R. S. *Appl. Phys. Lett.* **1974**, *24*, 65−68.

DOI: 10.1021/ic502939g
Inorg. Chem. 2015, 54, 2772−2779